JOURNAL OF CATALYSIS **160,** 269–278 (1996)
ARTICLE NO. 0145

Turnover Rate Enhancement of Reforming Reactions on Polycrystalline Pt–Ir Foils

Adrian L. Bonivardi,[1] Fabio H. Ribeiro,* and Gabor A. Somorjai

*Department of Chemistry, University of California at Berkeley, Berkeley, California 94720; and *Center for Advanced Materials, Materials Sciences Division, Ernest Orlando Lawrence Berkeley National Laboratory, Berkeley, California 94720*

Received August 29, 1995; revised December 18, 1995; accepted January 4, 1996

The reactions of *n*-hexane over bimetallic Pt–Ir polycrystalline foils were studied at 720 K, H_2/*n*-hexane = 67, and a total pressure of 0.9 MPa. The addition of Ir to Pt increases the hydrogenolysis turnover rate by up to two orders of magnitude and decreases the dehydrogenation turnover rate to 1-hexene by up to one order of magnitude. The rates of isomerization to 2- and 3-methylpentane and cyclization to methylcyclopentane show a volcano-type correlation when plotted against the surface Ir composition. The maximum rate occurs at a surface composition of Pt_2Ir and the rate is about three times higher than the rate for pure Pt. Addition of sulfur to the surface decreases the rates for isomerization, cyclization, and especially the rate for hydrogenolysis, resulting in a substantial decrease in the initial selectivity for hydrogenolysis. However, sulfur addition increases the dehydrogenation rates for the monometallic and bimetallic surfaces. It is observed that Pt–Ir shows a surface chemistry for the reactions of *n*-hexane similar to the surface chemistry of Pt when the bimetallic surface is sulfided. The turnover rates, however, are higher for Pt_2Ir than for Pt in the presence and absence of sulfur.

INTRODUCTION

The reforming of naphtha is one of the largest volume processes in the petroleum industry. The catalyst consists of either Pt–Re, Pt–Sn, or Pt–Ir clusters supported on a high surface area chlorinated alumina. The bimetallic Pt–Ir and Pt–Re catalysts have shown a superior performance, higher activity and, much improved activity maintenance over the monometallic first generation Pt catalysts (1). For this reason it is important to understand the role of the second metal. Of these three systems, Pt–Ir seems to have the highest rate per unit of volume of packed bed for a similar metal loading (2, 3). In addition, the reforming process can be more effective by using the Pt–Ir catalyst in the tail zone of a reforming unit for the better dehydrocyclization of paraffins of supported Pt–Ir versus Pt (1, 4).

[1] Present address: INTEC, Güemes 3450, 3000 Santa Fe, Argentina.

The advantages of these multimetallic systems are on their higher stability to deactivation and higher rates of reaction. A number of explanations for the increased stability are proposed. Cartel *et al.* (2) suggested that the lower rate of deactivation of Pt–Ir is due to a lower rate of carbonaceous deposits due to the higher rate of hydrogenolysis while Ramaswany *et al.* (5) suggested that the greater stability is due to a decreased rate of dehydrogenation on Pt–Ir catalysts. In our studies we found no evidence that Pt–Ir is more stable than Pt. However, our studies were geared to study the higher rates of Pt–Ir catalysts as compared to other Pt-based reforming catalysts. This increased activity seems to be one of the great commercial advantages of this system since production can be increased by changing to Pt–Ir catalyst on existing units instead of building new units.

Our approach to understand the role of the second metallic component has been to study the bimetallic system without the interference of the alumina support in the same way as we did before for Pt–Re (6). The model reaction for studying catalytic naphtha reforming is the conversion of *n*-hexane in the presence of excess hydrogen to other molecules by reactions involving dehydrogenation, isomerization, cyclization, and hydrogenolysis. We used a model catalyst system that consists of a polycrystalline Pt or Ir foil of small ($\sim$1 cm^2) surface area. Iridium was deposited on to Pt foil from a pulsed metal plasma gun; or conversely, Pt was deposited on an Ir foil in the same manner. The surface concentration of the two metals was determined by Auger electron spectroscopy (AES) and by the *n*-hexane dehydrogenation reaction which is particularly sensitive to Pt coverage. Then the bimetallic system was sulfided, both by sulfur deposition and by the addition of thiophene during the *n*-hexane reaction.

The presence of sulfur on the metal surface markedly reduced the hydrogenolysis activity of Ir (by two orders of magnitude). The rates and selectivities were the same whether Ir was deposited on Pt or Pt was deposited on Ir, indicating that the surface composition of the bimetallic

0021-9517/96 $18.00

system has equilibrated. The isomerization, cyclization, and dehydrogenation activity of the sulfided catalyst peaks at a surface composition of Pt_2Ir. Thus, sulfided Pt–Ir shows a Pt-like chemistry but it shows higher rates than pure Pt. The advantage of this system is that with this catalyst a higher production per volume of reactor can be achieved (increased production) or the catalyst can be operated at a lower temperature, resulting in lower deactivation rates.

EXPERIMENTAL METHODS

Experiments were carried out in an ultrahigh vacuum (UHV) chamber equipped with an AES, a metal vapor vacuum arc plasma gun (MEVVA), an electrochemical sulfur source, and an internal isolation reaction cell. The reaction cell was connected to an external gas recirculation loop forming a well-stirred batch reactor which can operate at pressures up to 2 MPa (7).

Sample Preparation

Iridium or platinum polycrystalline foils were used as starting materials to prepare the catalysts. Both foils were 0.0076 cm thick and of 99.95% purity. The sample (approx. 0.5 cm^2) was mounted to a rotary copper manipulator through Au–Ir (Ir foil) or Au–Pt (Pt foil) rods. The sample could be heated resistively, and the temperature measured by a chromel–alumel thermocouple spot welded to the edge of the foil.

Samples were cleaned by cycles of vacuum annealing (up to 1100 K for Ir, and 1200 K for Pt, at 1.3×10^{-7} Pa), heating in oxygen (up to 800 K at 6.7×10^{-5} Pa), and Ar ion sputtering (at 298 K and 8.0×10^{-3} Pa). These cycles were continued until the surface was certified clean by AES. The predominant impurities were Ca, Fe, K, O, S, and C on the Ir foil and Ca, O, S, and C on the Pt foil.

Bimetallic surfaces (Pt–Ir). Platinum–iridium bimetallic surfaces were prepared by depositing submonolayers to multilayers of Pt (Ir) on the Ir (Pt) foil with the MEVVA source operating in a pulse mode. A description of the principle of operation of this source has been previously reported by Kim *et al.* (8). Auger uptake curves were used to determine the amount of Pt (Ir) deposited at 298 K. After depositing the desired amount of platinum or iridium, the sample was annealed to 800 K for over 1 min before closing the reaction cell. This procedure assured a thermally stable bimetallic surface and will be described in more detail below.

Presulfided bimetallic surfaces (Pt–Ir–S). To prepare the presulfided samples, sulfur was vacuum deposited at 298 K using a electrochemical sulfur source described elsewhere (9). The bimetallic surfaces were covered by the saturation amount of sulfur and then annealed at 800 K (at 1.3×10^{-7} Pa, during 1 min). The amount of sulfur remaining was quantified by AES.

Catalytic Testing

A typical procedure was as follows. The sample was enclosed in the reaction loop where *n*-hexane (Fluka, purity >99.7%) and hydrogen (Matheson, purity 99.9995%) were fed sequentially, in this order, into the reactor. The reaction mixture was recirculated for 20 min before ramping the temperature of the sample to 720 K at 30 K s^{-1}. Additional experiments were performed to confirm that the order of addition of the reactants did not affect the reaction rate measurements. The reaction mixture was analyzed by gas chromatography with a flame ionization detector (HP 5890). The sample was injected at 16-min intervals by a gas sampling valve and separated by a PONA column (HP, 50 m $\times$ 0.2 μm $\times$ 0.5 μm film thickness).

Some experiments involved the addition to the reaction mixture of thiophene (10, 50, and 100 ppm) only over presulfided samples. In these cases, thiophene vapor from a solution of 600 ppm thiophene in *n*-hexane was added before feeding the reaction loop with *n*-hexane and H_2.

All reactions were run at 720 K with a H_2/*n*-hexane ratio of 67 and at a total pressure of 0.9 MPa. Under these conditions the main products analyzed were C_1–C_5 hydrocarbons (hydrogenolysis), 1-hexene (dehydrogenation), methylcyclopentane (MCP, cyclization), and 2-methylpentane and 3-methylpentane (2-mP and 3-mP, isomerization).

Since a batch reactor was used, kinetic data were obtained in the form of total accumulated product vs time plots. Initial reaction rates were determined from the initial slopes of these curves. The total conversion of *n*-hexane was always lower than 2% except for the clean Ir surface where the total conversion after 2 h of reaction was as high as 8%.

Initial turnover rates (TORs) were calculated per total number of metallic surface atoms, assuming a surface atom density of 1×10^{15} atom/cm^2 for the sulfided and nonsulfided samples (10). Therefore the TORs reported in this work are nominal TORs.

The initial selectivity to a particular product is defined as the ratio of moles of *n*-hexane converted to that product to the total moles of *n*-hexane converted and was calculated from the initial TORs.

The amounts of sulfur and carbon on the surface after 2 h of reaction were determined by AES. It was assumed that the calibration values for S/Pt(111) and C/Pt(111) obtained under similar experimental conditions remain valid for these experiments (11, 12).

In separated experiments it was verified that the convoluted Pt 237 eV and Ir 231 eV Auger signals of clean surfaces is constant with the iridium content. Thus, this convoluted signal was used as a reference to estimate the relative

concentrations of sulfur and carbon over the bimetallic surfaces.

RESULTS

Calibration of the Surface Composition of Pt on Ir Foil by Auger Spectroscopy

The Auger spectra of Pt and Ir overlap throughout the entire energy range. The range most suitable for analysis of surface concentrations is between 45 and 90 eV where the Auger electrons are very surface sensitive. In this energy range, the contribution to the total Auger signal by an atom at least 10 monolayers (ML) deep is less than 0.7% for Pt or Ir (13, 14). Therefore, we employed the decomposition and the normalization procedure of the Auger signal of Pt at 65 eV and Ir at 56 eV described by Sachtler *et al.* (15).

The normalized Auger signal intensity of Pt vs the number of pulses of Pt (from the MEVVA source) was used to calibrate the amount deposited over an Ir foil at room temperature (Fig. 1). Equidistant breaks of the curve are indicative of a Frank–van der Merwe or layer-by-layer growth mode for the first ($\theta = 1$ ML) and second monolayer ($\theta = 2$ ML) of Pt over an Ir foil (16). The same type of Auger signal vs number of pulses plot was observed when depositing Ir on a Pt foil at room temperature (Fig. 1).

The effect of annealing on the Auger signals of both metal adlayers was also studied since the catalytic activity of the bimetallics was determined after annealing of the sample. The normalized Pt Auger signal for half monolayer platinum on iridium is unchanged and identical to the initial value when the sample is annealed at 720 K for 2 h. Moreover, the annealing at 800 K for 4 min produces the same result. This suggests that island formation and/or the diffusion of Pt into the Ir bulk (foil) are not occurring and

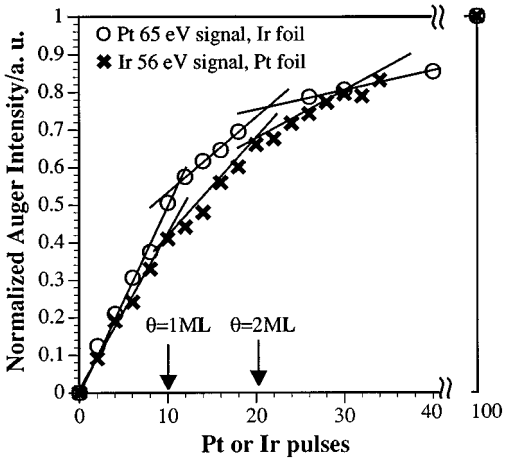

FIG. 1. Normalized Auger intensity of Pt 65 eV and Ir 56 eV signals vs number of Pt or Ir pulses on Ir or Pt foil, respectively. Deposition at 298 K.

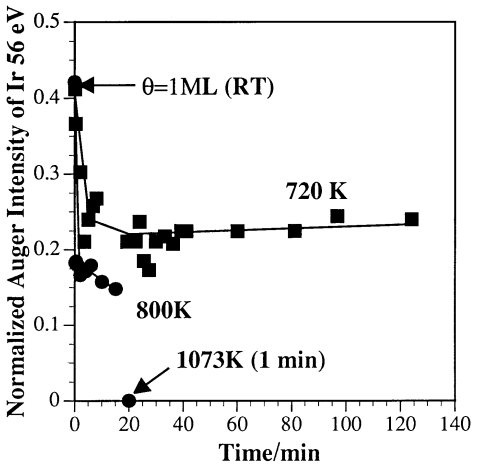

FIG. 2. Normalized Auger intensity of Ir 56 eV signal as a function of heating time at 720, 800, and 1073 K after depositing 1 ML Ir on Pt foil at 298 K.

the Auger calibration at 298 K was used to determine the surface composition of the bimetallic surfaces using an iridium foil. Thus, we defined the fraction of exposed Ir atoms (hereafter, FE_{Ir}) as the ratio of the number of Ir surface atoms to the total number of surface atoms. Hence, $0 \leq FE_{Ir} \leq 1$ and $FE_{Ir} = 1$ when $\theta \geq 1$ ML.

However, Fig. 2 indicates that annealing of one monolayer Ir deposited on Pt foil results in a decrease of the Ir Auger signal. At 720 K the intensity of the Auger signal decreases and after 20 min levels off. At higher temperature (800 K) the iridium signal is strongly attenuated and with continued heating (1073 K) it completely disappears.

Platinum surface segregation in Pt–Ir alloys is a well known phenomenon (17, 18). Agreement between experimental results and theoretical calculations has also been reported (19, 20). Therefore, one can conclude that after heating the Pt foil with Ir deposited on the surface, the Pt and Ir atoms will diffuse, resulting in a Pt surface enrichment. The opposite, the migration of Ir to the surface after heating the Ir foil with Pt deposited on the surface, is certainly not to be expected.

Consequently, the Auger calibration at 298 K is suitable only for the determination of FE_{Ir} (the fraction of Ir atoms on the surface) when depositing platinum on an iridium foil. Another method must be applied when using iridium on a platinum foil.

Calibration of the Surface Composition of Ir on Pt Foil by the Dehydrogenation of n-Hexane to 1-Hexene

Direct calibration of the fraction of exposed iridium atoms on an unsulfided Pt foil was accomplished with the dehydrogenation reaction of *n*-hexane to 1-hexene taking advantage of the fact that the rates over Pt and Ir are very different. Dehydrogenation–hydrogenation reactions are

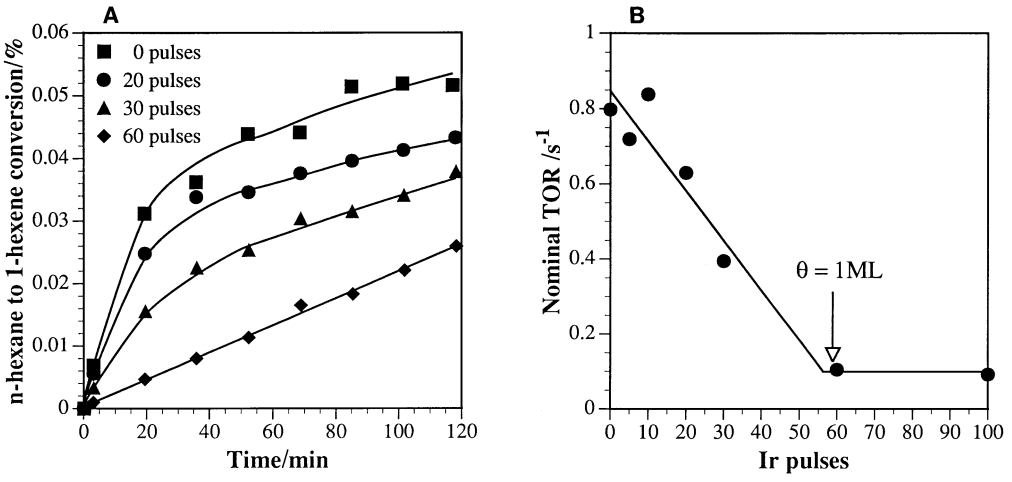

FIG. 3. (A) Conversion vs reaction time and (B) initial nominal turnover rate for *n*-hexane dehydrogenation to 1-hexene vs number of Ir pulses on clean Pt foil after annealing at 800 K. Reaction conditions: H_2/*n*-hexane = 67, T = 720 K, P_{total} = 0.9 MPa.

known to be structure insensitive or nondemanding reactions (21) and are thus strictly proportional to the amount of metallic sites on the surface. The percentage conversion of *n*-hexane to 1-hexene as a function of the reaction time (H_2/*n*-hexane = 67, 0.9 MPa, and 720 K) is depicted in Fig. 3A for different numbers of Ir pulses deposited over a Pt foil. It is worthwhile to pointout that the equilibrium conversion of *n*-hexane to 1-hexene is about 0.065% under these experimental conditions. Thus, it was possible to verify that the temperature measured by the thermocouple was correct (6, 22).

The initial nominal TORs for this reaction were calculated from the curves in Fig. 3A and plotted against the number of Ir pulses in Fig. 3B. A linear decrease in the dehydrogenation activity, from 0.85 s^{-1} for pure Pt to 0.1 s^{-1} for pure Ir, is observed, with the later TOR value reached after depositing approximately 60 Ir purses (~6 monolayers) over the Pt foil and annealing at 800 K. Assuming that a site involving no more than one atom of Pt is required to carry out this dehydrogenation reaction (23), the fraction of exposed iridium atoms (FE_{Ir}) on a Pt foil is calculated as the number of Ir pulse divided by 58 (value obtained by linear regression).

Turnover Rate and Selectivity of the Clean Pt–Ir Bimetallic System for n-Hexane Conversion

The effect of the metallic surface composition on the turnover rates and selectivities for *n*-hexane hydrogenolysis ($\Sigma_{<C6}$), dehydrogenation (1-hexene), isomerization (2-mP and 3-mP), and cyclization (MCP) are shown in Figs. 4 and 5. It is noted that the catalytic properties of Pt–Ir bimetallic surfaces are the same when an Ir or a Pt foil are used as substrates. Thus, the above different calibration methods of surface composition are consistent.

The TOR values for *n*-hexane hydrogenolysis on Pt–Ir bimetallic surfaces are plotted in Fig. 4 together with a fitting curve which is proportional to $(FE_{Ir})^2$. As the Ir content on Pt is increased, the hydrogenolysis activity goes from ~2 s^{-1} for clean platinum to 100 s^{-1} for pure iridium at 720 K, 0.9 MPa total pressure, and *n*-hexane/H_2 = 67. Since it is well documented that hydrogenolysis is a structure-sensitive reaction (24), a simple interpretation of the agreement between the curve and the points is to assume that the *n*-hexane hydrogenolysis requires two or more adjacent Ir atoms, that Pt has a much lower activity, and that the activation energy and the reaction mechanism are the same

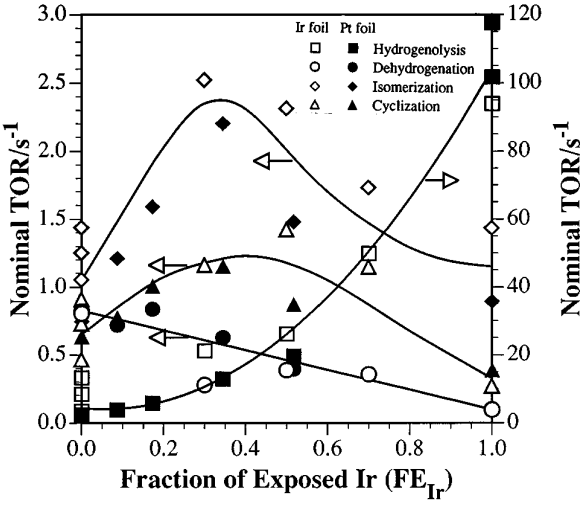

FIG. 4. Initial nominal turnover rate for *n*-hexane hydrogenolysis ($\Sigma_{<C6}$), dehydrogenation (1-hexene), isomerization (2-mP and 3-mP), and cyclization (MCP) vs fraction of exposed Ir atoms using Pt and Ir foils, without sulfur. Reaction conditions: H_2/*n*-hexane = 67, T = 720 K, P_{total} = 0.9 MPa.

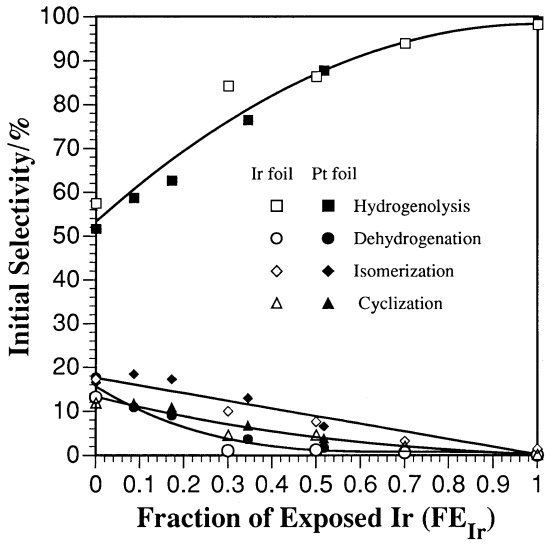

FIG. 5. Initial selectivity for *n*-hexane hydrogenolysis ($\Sigma_{<C6}$), dehydrogenation (1-hexene), isomerization (2-mP and 3-mP), and cyclization (MCP) vs fraction of exposed Ir atoms using Pt and Ir foils, without sulfur. Reaction conditions: H_2/*n*-hexane = 67, $T = 720$ K, $P_{total} = 0.9$ MPa.

for different surface compositions. This hypothesis is supported by the results of Foger and Anderson (25, 26) for the hydrocarbon hydrogenolysis in C_2-units mode on iridium surfaces.

If Ir were forming islands or patches over the Pt foil (or Pt on the Ir foil), we would have expected a linear increase of the hydrogenolysis activity as a function of the FE_{Ir} rather than the observed quadratic dependence (27). Thus, our results not only confirm the foreseen higher hydrogenolysis activity of iridium (28) and provide some evidence about the type of ensemble required, but also give an indication of the homogeneity of the surface composition of the samples prepared in this study.

The other reactions of *n*-hexane show different patterns of activity than hydrogenolysis. Figure 4 illustrates the synergetic effect of Ir on Pt for *n*-hexane isomerization and cyclization under the same experimental conditions. The turnover rates for these reactions are about the same on clean Pt and Ir. As the FE_{Ir} is changed, however, a maximum in the rate is observed. When about one-third of Ir covers the surface the rate of isomerization is 2.5 higher than for clean monometallic surfaces. The rate of MCP formation passes also through a maximum at approximately the same surface composition.

A linear loss of activity for *n*-hexane dehydrogenation as the fraction of exposed Ir increases is observed using both foils when sulfur was absent (Fig. 4). Furthermore, this was confirmed in a separate experiment with the decrease of the TOR for the dehydrogenation of cyclohexane to benzene on a nonsulfided Pt–Ir bimetallic sample ($FE_{Ir} = 0.5$) as compared to nonsulfided Pt (H_2/cyclohexane = 30, $P_{total} = 0.42$ MPa, $T = 573$ K). This is also consistent with results of dehydrogenation of cyclohexane and 1,1,3-trimethylcyclohexane for nonsulfided Pt and Pt–Ir catalysts (5, 29, 30).

The turnover rate for hydrogenolysis on clean Ir is at least two orders of magnitude higher than that for the other reforming reactions (Fig. 4). As a consequence, the *n*-hexane hydrogenolysis selectivity on a clean iridium foil is approximately 100% since the selectivities for dehydrogenation, isomerization, and cyclization strongly decrease with increasing Ir content and are negligible on clean iridium (Fig. 5). The addition of sulfur changes this selectivity drastically.

Turnover Rate and Selectivity Changes of the Pt–Ir Bimetallic System as a Function of Sulfur Coverage

The effect of sulfur content as a function of the fraction of exposed iridium atoms on the activity for *n*-hexane hydrogenolysis and dehydrogenation is shown in Fig. 6. The experimental reaction conditions are the same as those in Figs. 4 and 5. Representative data for the surfaces with no sulfur are also included in Fig. 6 for comparison.

The presulfiding process on iridium decreases the turnover rate for hydrogenolysis by more than one order of magnitude as compared to the clean metal (Fig. 6). Further addition of sulfur as thiophene to a presulfided bimetallic iridium surfaces reduces the initial nominal turnover rate for hydrogenolysis even more since thiophene maintains the sulfur surface concentration during the reaction (see below).

However, presulfided iridium shows a turnover rate for dehydrogenation similar to that of platinum without sulfur

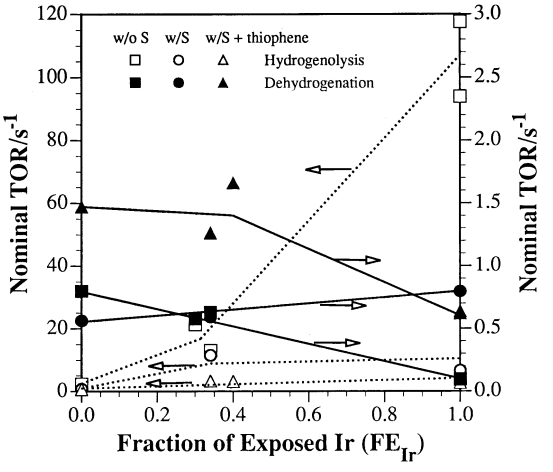

FIG. 6. Initial nominal turnover rate for *n*-hexane hydrogenolysis ($\Sigma_{<C6}$), and dehydrogenation (1-hexene) vs fraction of exposed Ir atoms using Pt and Ir foils, without presulfiding the samples (w/o S), presulfiding (w/ S) and presulfiding and adding 10 ppm of thiophene (w/S + thiophene). Reaction conditions: H_2/*n*-hexane = 67, $T = 720$ K, $P_{total} = 0.9$ MPa.

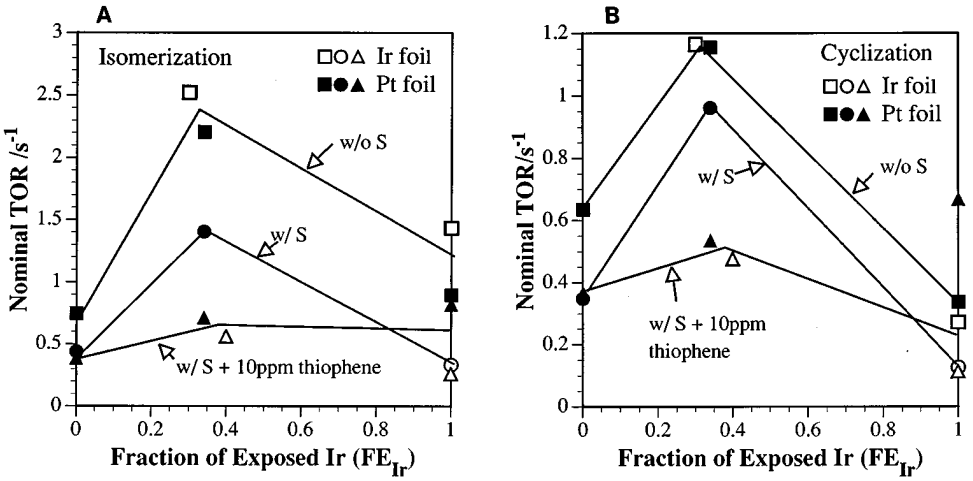

FIG. 7. (A) Initial nominal turnover rate for *n*-hexane isomerization (2-mP and 3-mP) and (B) cyclization vs fraction of exposed Ir atoms using Pt and Ir foils, without presulfiding the samples, presulfiding, and presulfiding and adding 10 ppm of thiophene. Reaction conditions: H_2/*n*-hexane = 67, $T = 720$ K, $P_{total} = 0.9$ MPa.

(Fig. 6). Further addition of sulfur as thiophene maintains the sulfided bimetallic surface as active as presulfided platinum for *n*-hexane dehydrogenation under the same experimental conditions. This is probably related to the fact that sulfided Ir is a more active catalyst for butene hydrogenation than sulfided platinum (31), suggesting the greater dehydrogenating activity of sulfided Ir. It can also be observed in Fig. 6 that in general the addition of sulfur increases the rates for dehydrogenation for pure Pt and Ir, as observed before by Apesteguía and Barbier (32). In other words, and opposite to what occurs to the rate for hydrogenolysis, structure-insensitive reactions like hydrogenation–dehydrogenation are enhanced by modifying the Pt surface with iridium and sulfur.

Figures 7A and 7B show the variation of the turnover rates for isomerization and cyclization as a function of the metallic surface composition (FE_{Ir}) versus sulfur content. Again, representative data of surfaces without sulfur are included in this figure for comparison. Presulfided Pt–Ir bimetallic surfaces ($FE_{Ir} \sim 0.35$) are still 2-fold and 1.5-fold more active for isomerization and cyclization, respectively, than clean platinum. Moreover, presulfiding and the addition of 10 ppm of thiophene do not produce a substantial reduction of the rate for these reactions as it happens for hydrogenolysis, which was indeed the most affected reaction by sulfur poisoning (Fig. 6).

A typical accumulated product versus time plot for *n*-hexane cyclization as a function of sulfur content on a bimetallic surface ($FE_{Ir} = 0.35$) is shown in Fig. 8. The initial cyclization rate for the presulfided surface is lower than that for the clean surface, but higher conversion values are reached in the first case with time. It is clear that sulfur decreases the deactivation rate of the catalyst. Moreover, it is possible to end with the same *n*-hexane conversion, or MCP concentration, using the clean or the presulfided and thiophene added (10 ppm) bimetallic surface. It is noted as well in Fig. 8 that a continuous increase in the cyclization rate with time with further thiophene additions (50 and 100 ppm) occurs.

A similar behavior was observed for isomerization and other surface compositions. Thus, two opposite trends are responsible for the catalytic behavior observed. One is the surface polymeric carbon deposition and the other is the surface sulfur removal with time, as discussed bellow.

Figures 9 and 10 show the effect of sulfur on the initial selectivities to hydrogenolysis, dehydrogenation, isomerization and cyclization as a function of the metallic surface composition. Again, the strong poisoning effect of sulfur

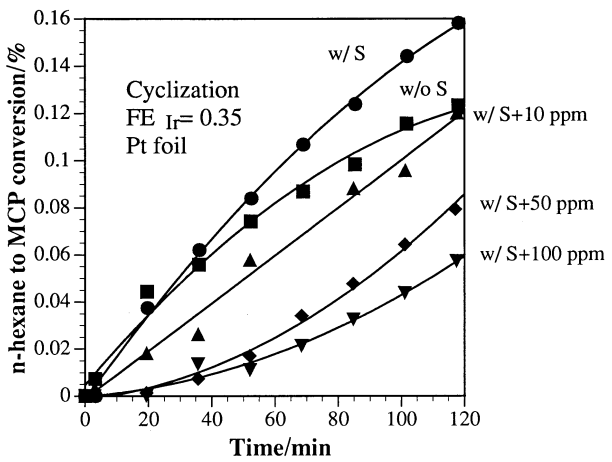

FIG. 8. Conversion to MCP vs reaction time for a sample with $FE_{Ir} = 0.35$ (Pt foil) as a function of sulfur content. Reaction conditions: H_2/*n*-hexane = 67, $T = 720$ K, $P_{total} = 0.9$ MPa.

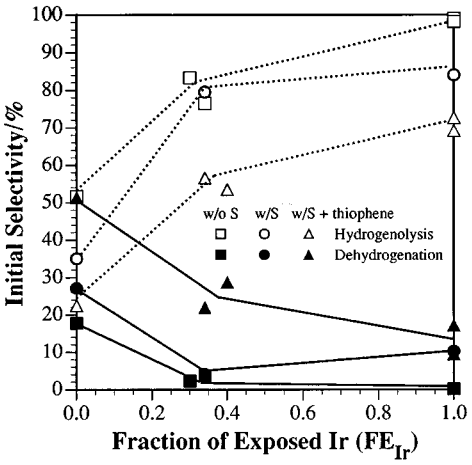

FIG. 9. Initial selectivity for *n*-hexane hydrogenolysis ($\Sigma_{<C6}$) and dehydrogenation (1-hexene) vs fraction of exposed Ir atoms using Pt and Ir foils, without presulfiding the samples (w/o S), presulfiding (w/ S), and presulfiding and adding 10 ppm of thiophene (w/ S + thiophene). Reaction conditions: H_2/*n*-hexane = 67, T = 720 K, P_{total} = 0.9 MPa.

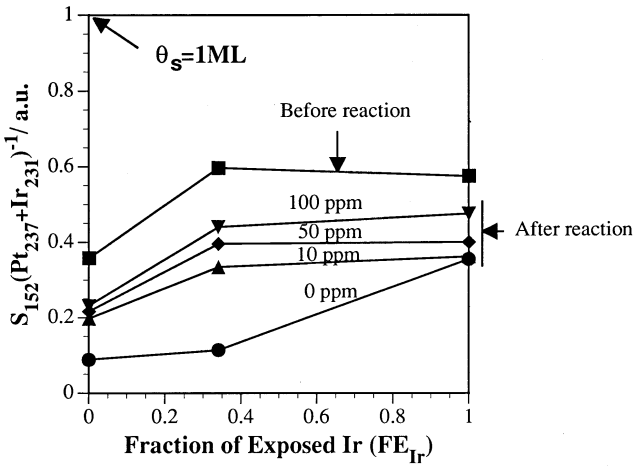

FIG. 11. Surface sulfur content on presulfided samples before and after 2 h of reaction (H_2/*n*-hexane = 67, T = 720 K, P_{total} = 0.9 MPa) with different thiophene concentrations, plotted as the ratio between S 152 eV and the (Pt 237 eV + Ir 231 eV) Auger peaks vs fraction of exposed Ir atoms.

on the hydrogenolysis reaction is observed in Fig. 9. Sulfur and thiophene lower the selectivity to hydrogenolysis products ($\Sigma_{<C6}$) by 40–50% compared to the clean surfaces, while improving the selectivity to 1-hexene (Fig. 9). The isomerization and cyclization selectivities, however, decrease as the amount of Ir is increased (Figs. 10A and 10B). It is concluded that under the presence of sulfur Pt–Ir catalytic surfaces approach the behavior of Pt surfaces.

Sulfur and Carbon Surface Concentrations on the Pt–Ir Bimetallic Catalysts

Figure 11 shows the sulfur coverage on the metallic surfaces before and after reaction versus the metallic surface composition. The sulfur coverage is expressed as the ratio of the S 152 eV Auger signal to the convoluted Pt 237 eV and Ir 231 eV Auger signals.

The sulfur coverage (θ_S) on the metallic surfaces before starting the reaction is shown in the upper curve in Fig. 11. In this case the sulfur coverage on a Pt polycrystalline foil is 0.35 ML which is in good agreement with the value expected for $(\sqrt{3} \times \sqrt{3})$ R 30°-S/Pt(111) (θ_S = 0.33 ML) obtained for similar preparation conditions (9, 11). This is expected since polycrystalline foils of fcc metals have a large surface fraction of (111) planes (33).

The sulfur coverage on iridium before reaction, however, is 0.6 ML because S binds more strongly to Ir than to Pt. This last value is also consistent with that reported by Barbier

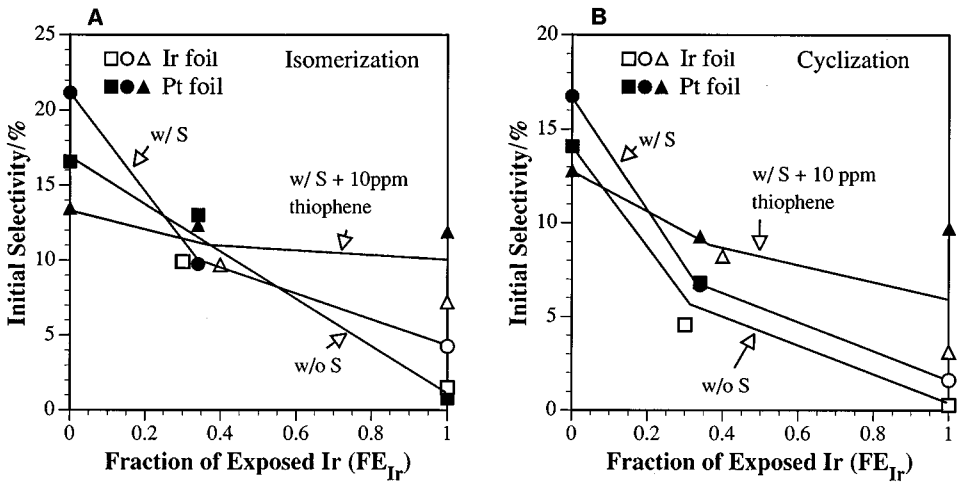

FIG. 10. Initial selectivity for *n*-hexane (A) isomerization (2-mP and 3-mP) and (B) cyclization (MCP) vs fraction of exposed Ir atoms using Pt and Ir foils, without presulfiding the samples, presulfiding, and presulfiding and adding 10 ppm of thiophene. Reaction conditions: H_2/*n*-hexane = 67, T = 720 K, P_{total} = 0.9 MPa.

et al. for irreversible adsorbed sulfur at 773 K on low dispersed iridium catalysts, i.e., large crystallites with surface structure similar to a foil surface (34).

In the same figure it is noted that Pt–Ir bimetallic surface is able to maintain the same amount of adsorbed sulfur as iridium ($\theta_s = 0.6$ ML). One possible explanation for this observation could be the structure-sensitive adsorption of sulfur on Ir, i.e., small Ir ensembles have greater sensitivity to sulfur than large ensembles (34).

After 2 h of reaction the remaining sulfur amount on the surfaces was always lower than the initial one, indicating that sulfur removal occurs with reaction time. However, the added thiophene increases the surface sulfur amount at the end of the reaction (Fig. 11). This effect is stronger on Ir-containing surfaces than on pure platinum probably due to the higher thiophene dehydrosulfurization activity and the strong affinity of iridium to sulfur (31).

The other element present over presulfided surfaces after reaction was carbon. The relative amounts of deposited carbon were also followed by Auger spectroscopy. The ratio of C 272 eV to the convoluted Pt 237 eV and Ir 231 eV Auger signals versus the thiophene concentration is shown in Fig. 12. The deposited carbon amount over the presulfided surfaces after reaction decreases no more than 25% as the concentration of thiophene is increased regardless of the iridium surface concentration.

We also found that for surfaces without sulfur, the amount of carbon was independent of the FE_{Ir} and approximately one monolayer (not shown in the figure).

In summary, the addition of iridium to the platinum surface increases the sulfur surface concentration on the catalysts. Thiophene is essential to keep the sulfur surface concentration of the presulfided samples.

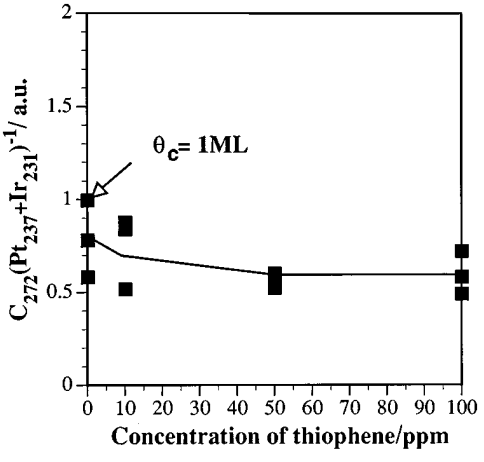

FIG. 12. Surface carbon content accumulated on presulfided samples after 2 h of reaction (H_2/*n*-hexane = 67, $T = 720$ K, $P_{total} = 0.9$ MPa) with different thiophene concentrations, plotted as the ratio between the C 272 eV and the (Pt 237 eV + Ir 231 eV) Auger peaks vs thiophene concentration.

DISCUSSION

Iridium as a Hydrogenolysis Catalyst

It has been shown that the turnover rate for the hydrogenolysis of *n*-hexane over Pt–Ir surfaces increases with the fraction of exposed Ir on the surface. A large difference in activity between the two clean metals was observed, with Ir some 50 times more active than Pt (Fig. 4). This result is in agreement with those reported by Garden *et al.* (35) for the hydrogenolysis of linear hydrocarbons. These authors found that at 473 K and hydrogen/hydrocarbon ratio of 10, Ir is 100 and 60 times more active than Pt for *n*-butane and *n*-pentane hydrogenolysis, respectively.

Following this reasoning, we would expect a similar increase for the *n*-heptane hydrogenolysis activity. However, an increase by five orders of magnitude was observed for the hydrogenolysis of *n*-heptane on Ir over Pt by Carter *et al.* (36) using a much lower hydrogen/hydrocarbon ratio. This result can be explained if we take into account the high negative order in hydrogen found previously for hydrogenolysis of hydrocarbons on metals (25, 37). Foger and Anderson have found that the hydrocarbon C_p–C_s and C_s–C_s (p, primary; s, secondary) bond cleavage on Ir occurred with the same activation energy (170 kJ mol^{-1}) and, provided the hydrogen pressure was kept high enough, the reaction rates were proportional to $P_{HC}P_{H_2}^{-3}$ (25, 26). In the case of Pt the rate for hydrogenolysis is proportional to $P_{HC}\ P_{H_2}^{-1}$ (37). Consequently, the activity values reported by Carter *et al.* corrected to 720 K, H_2/*n*-heptane = 67 and 0.9 MPa give an expected ratio of the activity for *n*-heptane hydrogenolysis on Ir over Pt of ~ 20, in good agreement with our results for *n*-hexane.

Thus, the high activity of iridium for hydrogenolysis makes this metal inappropriate for use as a reforming catalyst. However, as it has been shown, modification of the surface by sulfur leads to suppression of the hydrogenolysis activity and selectivity resulting in an increase in the yield to useful reforming products on a Pt–Ir bimetallic surface. The same conclusions were found for supported Pt/Ir catalysts (38).

Turnover Rate Enhancement by Addition of Ir to Pt

It is important now to recall what are the most remarkable characteristics of Pt–Ir bimetallic surfaces. Both platinum and iridium give similar TOR values for the isomerization of *n*-hexane to 2-mP and 3-mP or its cyclization to MCP. Nevertheless, the platinum–iridium bimetallic surface with the atom fraction of exposed iridium of about 0.35 has a higher activity for isomerization and cyclization (Figs. 4 and 7). This maximum in activity for *n*-hexane isomerization and cyclization could be explained by a change or simply an acceleration in the rate determining step.

It has been reported that the isomerization of hexanes on Pt/Al_2O_3 occurs through two different mechanisms, i.e.,

the bond shift and cyclic mechanisms. The contribution of each mechanism depends strongly on the Pt dispersion (39). The properties of low dispersion Pt catalysts were simulated using Pt single-crystals and polycrystalline foils by Maire's group (33, 40) and they reported that the cyclic mechanism prevails over the bond shift mechanism, even when they competed. Moreover, Weisang and Gault (41) suggested that isomerization of hexanes on 10% Ir/Al_2O_3 and Ir sponge catalysts occurs only via a cyclic mechanism involving cyclopentadienyl species. Our results indicate that the TOR for isomerization of *n*-hexane is about the same on clean Pt and Ir and enhanced MCP formation accompanies enhanced production of 2- and 3-mP (Fig. 4). Thus, it does not seem possible to attribute the maximum in activity only to a change in the reaction mechanism, and the different surface composition may be responsible for changes in the rate-determining step of the reactions. At an Ir surface concentration of about 0.35 the number of Pt–Ir nearest neighbors are high and the number of Ir–Ir neighbors are low. This Pt–Ir site may have a higher isomerization activity by speeding the rate determining step: Ir sites can adsorb and dissociate hydrocarbons easily which then diffuse to the Pt sites where they can isomerize. Thus, Pt-rich catalysts cannot adsorb and dissociate fast enough and Ir-rich catalysts adsorb molecules too strongly (35) which cause higher hydrogenolysis rates (42). A similar argument was proposed by Haining *et al.* (43) to explain the maximum in the rate of *n*-butane hydrogenolysis on Pt–Re catalysts.

Using this hypothesis to understand the maximum in isomerization and cyclization activity seems more reasonable than invoking a decrease in the poisoning by coke deposition because: (i) this synergistic effect of Ir on Pt occurs with and without the presence of sulfur under our experimental conditions, i.e., whether or not deactivation exist (Fig. 8), and (ii) under severe deactivation conditions Pt–Ir–S is more active for isomerization and cyclization than Pt–S (740 K, H_2/*n*-hexane = 30, $P_{total} = 0.45$ MPa) (44).

The Pt–Ir Model System and the Behavior of the Supported Catalyst

In the foregoing sections we discussed activities and selectivities of the various mono and platinum–iridium bimetallic surfaces and the effect of sulfur on the catalytic properties of these systems.

Our experiments were performed at a temperature and pressure close to industrial reforming conditions but a higher hydrogen to hydrocarbon ratio had to be used in order to avoid severe poisoning by coke deposition, the more so as these are results at initial conditions obtained in a batch reactor. Moreover, in the industrial catalyst the highly dispersed metallic phase is supported on chlorinated alumina but is absent in our preparations. For these reasons, direct extrapolation and comparison of these results to the industrial system are not possible.

TABLE 1

Sum of the Nominal Turnover Rates (TOR) for Dehydrogenation, Isomerization, and Cyclization as a Function of the Bimetallic Surface Composition and Sulfur Content

Stoichiometry of the surface	Sum of the nominal TOR for dehydrogenation, isomerization, and cyclization (s^{-1})		
	w/o S	w/ S	w/ S + 10 ppm thiophene
Pt	2.2	1.6	2.2
Pt_2Ir	4.3	3.0	2.6
Ir	1.6	1.3	1.9

It has been reported, however, that Pt–Ir–S-supported catalysts are more active for dehydrocyclization and cracking reactions than Pt (2). Carter *et al.* (2) have observed that the rate of *n*-heptane dehydrocyclization per gram of catalyst (r_D, includes toluene and cycloalkanes) for 0.3% Pt–0.3% Ir/Al_2O_3 is higher than for 0.3% Pt/Al_2O_3 alone (data after 40 h on stream at 495°C, 14.6 atm, and hydrogen/*n*-heptane = 5/1). Assuming equivalent dispersions for both catalysts, the r_D of the their Pt–Ir bimetallic supported catalyst is still ~20% higher than supported Pt.

In our unsupported model systems and under our reaction conditions, benzene and cyclohexene were essentially absent because the reaction of MCP to benzene needs the acid sites of the alumina to take place (45, 46). However, the sum of the nominal TOR for dehydrogenation, isomerization, and cyclization on the platinum–iridium bimetallic surface (Pt_2Ir) is at least 18% higher than for platinum (Table 1). Thus, it is expected that the bimetallic catalyst will show a better performance.

Carter *et al.* (2) also reported that the rate of cracking of *n*-heptane (r_H, includes C_1–C_6) for their sulfided platinum–iridium bimetallic catalyst was twice as high as for supported Pt–S but similar to supported Ir–S. This is also the trend of our results. After presulfiding the samples and carrying out our experiments with 10 ppm of thiophene, the rates of *n*-hexane hydrogenolysis were similar for Pt–Ir–S and Ir–S systems but five times higher than that for Pt–S.

In addition, with all of our presulfided catalysts it was possible to reach the equilibrium concentration of the olefin by dehydrogenation in less than 2 h, suggesting that severe carbon poisoning can be ruled out (6). Also, the deactivation observed for nonpresulfided samples was decreased with the addition of small amounts of sulfur (see as an example Fig. 8). Bearing this in mind, it is difficult to accept that the stability of the Pt–Ir–S/Al_2O_3 catalysts is due to the lower rate of dehydrogenation on iridium (5) since Pt–Ir–S was as active as Pt–S for the dehydrogenation of *n*-hexane (Fig. 6), and more active for the dehydrogenation of cyclohexane (32) and hydrogenation of benzene (29).

In fact, our results do not point to a lower deactivation rate of Pt–Ir as compared to Pt, as shown for the Pt–Re

system (6). However, the higher TOR for isomerization and cyclization will result in a lower deactivation rate of the Pt–Ir system: when iridium and sulfur are added to platinum, the resulting Pt–Ir–S is a more active catalyst than clean platinum and lower temperatures of operation can be used with a subsequent lower deactivation rate.

CONCLUSIONS

Iridium has a much higher rate for hydrogenolysis than for isomerization, cyclization and dehydrogenation. The turnover rate for hydrogenolysis on iridium is two orders of magnitude higher than for platinum while the turnover rate for the reactions of isomerization and cyclization are about the same as the rates for platinum.

Sulfur addition to Ir-containing surfaces strongly inhibits the activity for *n*-hexane hydrogenolysis and sustains activity and selectivity for the other reforming reactions. Therefore, sulfur is necessary to poison the undesired reactions in an iridium containing catalyst.

The Pt–Ir bimetallic surface has a unique reforming catalytic property at a surface composition corresponding to Pt_2Ir: It shows higher activities for *n*-hexane isomerization and cyclization than pure platinum or iridium. This turnover rate enhancement remains for sulfided bimetallic surfaces. Thus, Pt–Ir–S acts as a more active Pt-like reforming catalyst.

A sulfided platinum–iridium catalyst can then be operated at a lower temperature than platinum with the same conversion level, which will result in a lower deactivation rate as compared to platinum. Thus, the combined effect of the addition of iridium and sulfur to platinum produces a better reforming catalyst.

ACKNOWLEDGMENTS

This work was supported by the Director, Office of Energy Research, Office of Basic Energy Sciences, Materials Sciences Division, of U.S. Department of Energy under Contract DE-AC03-76SF00098. A. L. Bonivardi acknowledges the financial support from CONICET (Consejo Nacional de Investigaciones Cientifícas y Técnicas) of Argentina.

REFERENCES

1. Sinfelt, J. H., *in* "Bimetallic Catalysts: Discoveries, Concepts, and Applications." Wiley, New York, 1983.
2. Carter, J. L., McVicker, G. B., Weissman, W., Kmak, W. S., and Sinfelt, J. H., *Appl. Catal.* **3**, 327 (1982).
3. Cecil, R. R., Kmak, W. S., Sinfelt, J. H., and Chambers, L. W., *Oil Gas J.* **70**, 50 (1972).
4. Sinfelt, J. H., U.S. patent 3,791,961 (1974).
5. Ramaswamy, A. V., Ratnasamy, P., Sivasanker, S., and Leonard, A. J., *in* "Procedings of the International Congress on Catalysis, 6th," (G. C. Bond, P. B. Wells, and F. C. P. Tompkins, Eds.), Vol. 2, p. 855, Chem. Soc., Letchworth, U.K., 1976.
6. Ribeiro, F. H., Bonivardi, A. L., Kim, C., and Somorjai, G. A., *J. Catal.* **150**, 186 (1994).
7. Kahn, O. R., Petersen, E. E., and Somorjai, G. A., *J. Catal.* **34**, 294 (1974).
8. Kim, C., Ogletree, D. F., Salmeron, M. B., Godechot, Y., Somorjai, G. A., and Brown, I. G., *Appl. Surf. Sci.* **59**, 261 (1992).
9. Heegemann, W., Meoster, K. H., Betchtold, E., and Hayek, K., *Surf. Sci.* **49**, 161 (1975).
10. Somorjai, G. A., *in* "Introduction to Surface Chemistry and Catalysis." Wiley, New York, 1994.
11. Kim, C., and Somorjai, G. A., *J. Catal.* **134**, 179 (1992).
12. Biberian, J. P., and Somorjai, G. A., *Appl. Surf. Sci.* **2**, 352 (1979).
13. Seah, M. P., and Dench, W. A., *Surf. Interface Anal.* **1**, 2 (1979).
14. Gallon, T. E., *Surf. Sci.* **17**, 486 (1969).
15. Sachtler, J. W. A., Van Hove, M. A., Biberian, J. P., and Somorjai, G. A., *Surf. Sci.* **110**, 19 (1981).
16. Argile, C., and Rhead, G. E., *Surf. Sci. Rep.* **10**, 277 (1989).
17. Kuijers, F. J., and Ponec, V., *Appl. Surf. Sci.* **2**, 43 (1978).
18. Hoernstroem, S. E., and Johansson, L. I., *Appl. Surf. Sci.* **27**, 235 (1986).
19. Ossi, P. M., *Surf. Sci.* **201**, L519 (1988).
20. Mukherjee, S., and Moran-Lopez, J. L., *Surf. Sci.* **188**, L742 (1987).
21. Boudart, M., *Adv. Catal.* **20**, 153 (1969).
22. Davis, S. M., Zaera, F., and Somorjai, G. A., *J. Am. Chem. Soc.* **104**, 7453 (1982).
23. Biloen, P., Dautzenberg, F. M., and Sachtler, W. M. H., *J. Catal.* **50**, 77 (1977).
24. Boudart, M., and Djéga-Mariadassou, G., *in* "Kinetics of Heterogeneous Catalytic Reactions." Princeton Univ. Press, Princeton, NJ, 1984.
25. Foger, K., and Anderson, J. R., *J. Catal.* **59**, 325 (1979).
26. Foger, K., and Anderson, J. R., *J. Catal.* **64**, 448 (1980).
27. Yang, O. B., Woo, S. I., and Ryoo, R., *J. Catal.* **137**, 357 (1992).
28. Sinfelt, J. H., *Adv. Catal.* **23**, 91 (1973).
29. Leclercq, G., Charcosset, H., Maurel, R., Bertizeau, C., Bolivar, C., Frety, R., Jaunay, D., Mendez, H., and Tournayan, L., *Bull. Soc. Chim. Belg.* **88**, 577 (1979).
30. Betizeau, C., Leclercq, G., Maurel, R., Bolivar, C., Charcosset, H., Frety, R., and Tournayan, L., *J. Catal.* **45**, 179 (1976).
31. Vissers, J. P. R., Groot, C. K., Van Oers, E. M., De Beer, V. H. J., and Prins, R., *Bull. Soc. Chim. Belg.* **93**, 813 (1984).
32. Apesteguia, C. R., and Barbier, J., *J. Catal.* **78**, 352 (1982).
33. Garin, F., Aeiyach, S., Legare, P., and Maire, G., *J. Catal.* **77**, 323 (1982).
34. Barbier, J., Marecot, P., Tifouti, L., Guenin, M., and Frety, R., *Appl. Catal.* **19**, 375 (1985).
35. Garden, D., Kemball, C., and Whan, D. A., *J. Chem. Soc. Faraday Trans. 1* **82**, 3113 (1986).
36. Carter, J. L., Cusumano, J. A., and Sinfelt, J. H., *J. Catal.* **20**, 223 (1971).
37. Garin, F., and Gault, F. G., *J. Am. Chem. Soc.* **97**, 4466 (1975).
38. Dees, M. J., and Ponec, V., *J. Catal.* **115**, 347 (1989).
39. Maire, G. L. C., and Garin, F., *in* "Catalysis: Science and Technology" (J. R. Anderson and M. Boudart, Eds.), Vol. 6, p. 161. Springer-Verlag, Berlin, 1984.
40. Dauscher, A., Garin, F., and Maire, G., *J. Catal.* **105**, 233 (1987).
41. Weisang, F., and Gault, F. G., *J. Chem. Soc. Chem. Commun.* **11**, 519 (1979).
42. Faro, A. C., and Kemball, C., *J. Chem. Soc. Faraday Trans. 1* **82**, 3125 (1986).
43. Haining, I. H. B., Kemball, C., and Whan, D. A., *J. Chem. Res. Synop.* **7**, 170 (1977).
44. Ribeiro, F. H., Bonivardi, A. L., and Somorjai, G. A., *Catal. Lett.* **27**, 1 (1994).
45. Mills, G. A., Heinemann, H., Milliken, T. H., and Oblad, A. G., *Ind. Eng. Chem.* **45**, 134 (1953).
46. Paál, Z., *in* "Catalytic Naphtha Reforming," (G. J. Antos, A. M. Aitani, and J. M. Parera, Eds.), p. 19. Dekker, New York, 1995.